

DOE/PC/94208--T4

THIRD TECHNICAL PROGRESS REPORT
APRIL, 1995
ON

**HYDRODYNAMIC MODELS FOR SLURRY BUBBLE COLUMN
REACTORS**

U.S. Department Energy Grant
DE-FG22-94PC94208

D.Gidaspow, Principal Investigator
Department of Chemical Engineering
Illinois Institute of Technology
Chicago, Illinois 60616

ABSTRACT

The objective of this investigation is to convert our "learning gas-solid-liquid" fluidization model into a predictive design model. The IIT hydrodynamic model computes the phase velocities and the volume fractions of gas, liquid and particulate phases. Model verification involves a comparison of these computed velocities and volume fractions to experimental values.

After a discussion of our research with the DOE-Air Products team in January, we decided to concentrate on the slurry configuration of interest to DOE-Air Products which has no recirculation of liquid. In such a system the gas is the continuous phase, rather than the liquid that we had used in our model in the past. We have built such a cold flow two dimensional plastic model. We have also changed our computer code. At the request of Air Products and DOE we have started a simulation of LaPorte RUN E-8.1 (1991) for production of methanol as described in the Air Products report sent to us. For isothermal operation, there is good mixing, and the preliminary results shown in this report indicate that we should obtain an agreement between the experiment and the simulations. A final report will be prepared upon completion of the simulation.

Diana Matonis, a Ph.D. candidate supported by an ITRI fellowship, has developed a three dimensional version of our G-L-S code which will be used in the present study.

"U.S. DOE PATENT CLEARANCE NOT REQUIRED PRIOR TO PUBLICATION OF THIS REPORT."

DISCLAIMER

This report was prepared as an account of work sponsored by an agency of the United States Government. Neither the United States Government nor any agency thereof, nor any of their employees, makes any warranty, express or implied, or assumes any legal liability or responsibility for the accuracy, completeness, or usefulness of any information, apparatus, product, or process disclosed, or represents that its use would not infringe privately owned rights. Reference herein to any specific commercial product, process, or service by trade name, trademark, manufacturer, or otherwise does not necessarily constitute or imply its endorsement, recommendation, or favoring by the United States Government or any agency thereof. The views and opinions of authors expressed herein do not necessarily state or reflect those of the United States Government or any agency thereof.

DISTRIBUTION OF THIS DOCUMENT IS UNLIMITED

MASTER

RECEIVED
USDOE/PETC
12/53

**SIMULATION OF SYNTHESIS OF METHANOL IN
AIR PRODUCTS AND CHEMICALS' SLURRY REACTOR
WITHOUT CIRCULATION OF SLURRY**

Yuanxiang Wu, Research Assistant
Dr. Dimitri Gidaspow, Principal Investigator
Department of Chemical Engineering
Illinois Institute of Technology
Chicago, IL 60616

INTRODUCTION:

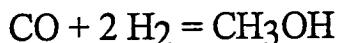
Air Products and Chemicals, Inc. produced methanol from syn-gas, a mixture of H_2 and CO, in the LaPorte pilot unit (1987, 1991, 1992). We are simulating this process using our multiphase code with the reaction of methanol. In our pervious report (1994a), the case of LaPorte RUN E-2-B(1987) was simulated. A good agreement with LaPorte's NDG concentrations of catalyst and the production of methanol was obtained. In the present report, RUN E-8.1(1991) is used. The major difference of this simulation from the pervious one is the absence of slurry circulation. Also upon request of Air Products and Chemical, Inc., we added the heat exchangers to the reactor.

The following difficulties in our simulation need to be mentioned:

1. Our multiphase code with reaction is only 2 dimensional. If the tube of the heat exchanger is put into the 2-D reactor, it must partition the 2-D reactor into 2 parts without connection. Therefore, a discontinuous heat exchanger is used in the simulation. A 3-D multiphase code with reaction needs to be developed. Diana Matonis, a Ph.D candidate, is developing a 3-D code.
2. In order to track the propagation of methanol formation inside the reactor, it is best to choose an initial state without any syn-gas (inert only such as N_2). Then the syn-gas is injected at zero time. We did this, but it takes a long computing time to reach product's steady state at the top outlet. This report only shows the results of the partial steady state.
3. A non-isothermal simulation was conducted first. But an extreme hot area was formed in the entrance (below the heat exchanger) in the very early computing time because of the accumulation of reaction heat. So, an isothermal simulation was conducted. The parameters of the heat generation and the temperature of the inlet gas need to be adjusted in a future run.

REACTION:

According to the report of Air Products and Chemical, Inc.(1991), RUN E-8.1 produced methanol only. The methanol dehydration and water shift reaction were very small. Therefore only methanol synthesis is considered here:



The methanol kinetic expression is chosen from DME report(1992):

$$r = k_f f_{\text{CO}}^{1/3} f_{\text{H}_2}^{2/3} \left(1 - \frac{f_{\text{MEOH}}}{K_{eq} f_{\text{CO}} f_{\text{H}_2}^2} \right)$$

MASS TRANSFER BETWEEN GAS AND LIQUID PHASE:

$$R_i = K_{Li} a (C_i^{g-L} - C_i^L)$$

From Viking Systems International's report and Ledakowicz et al(1984):
 $K_{Li} = 0.3--1.3$ (1/s). By using Henry's Law:

$$C_{Li}^{g-L} = \frac{f_i}{H_i}$$

Followings are expressions of Henry's constants from Graaf, G.H.(1988) for $T=210-260$ °C.

$$H_{\text{CO}} = 0.175 \exp(638/RT)$$

$$H_{\text{CO}_2} = 0.402 \exp(-6947/RT)$$

$$H_{\text{H}_2} = 0.0782 \exp(4875/RT)$$

$$H_{\text{CH}_3\text{OH}} = 1.49 \exp(-17235/RT)$$

$$H_{\text{H}_2\text{O}} = 0.33 \exp(-8633/RT)$$

HYDRODYNAMIC MODEL for multiphase flow with reaction and interfacial mass transports (D. Gidaspo 1994b).

Continuity equations:

$$\frac{\partial}{\partial t} (\epsilon_g \rho_g) + \nabla \cdot (\epsilon_g \rho_g V_g) = \dot{m}_g$$

$$\frac{\partial}{\partial t} (\epsilon_l \rho_l) + \nabla \cdot (\epsilon_l \rho_l V_l) = \dot{m}_l$$

$$\frac{\partial}{\partial t} (\epsilon_s \rho_s) + \nabla \cdot (\epsilon_s \rho_s V_s) = \dot{m}_s$$

$$\epsilon_g + \epsilon_l + \epsilon_s = 1$$

Momentum equations:

$$\frac{\partial}{\partial t} (\epsilon_g \rho_g V_g) + \nabla \cdot (\epsilon_g \rho_g V_g V_g) = -\nabla P_g - \epsilon_g \rho_g g + \nabla \cdot \tau_g + \beta_{sg} (V_s - V_g) + \beta_{lg} (V_l - V_g) + \dot{m}_g V_g$$

$$\frac{\partial}{\partial t} (\epsilon_l \rho_l V_l) + \nabla \cdot (\epsilon_l \rho_l V_l V_l) = -\nabla P_l - \epsilon_l \rho_l g + \nabla \cdot \tau_l + \beta_{lg} (V_g - V_l) + \beta_{ls} (V_s - V_l) + \dot{m}_l V_l$$

$$\frac{\partial}{\partial t} (\epsilon_s \rho_s V_s) + \nabla \cdot (\epsilon_s \rho_s V_s V_s) = -\nabla P_s - \epsilon_s \rho_s g + \nabla \cdot \tau_s + \beta_{sg} (V_g - V_s) + \beta_{ls} (V_l - V_s) - \dot{m}_s V_s$$

$$\dot{m}_s = 0 \quad \dot{m}_l = -\dot{m}_g = \epsilon_l \sum_{i=1}^N R_i M_i \quad i = H_2, CO, CO_2, CH_4, CH_3OH, H_2O$$

Shear stresses:

$$\nabla P_k = G(\epsilon_k) \nabla \epsilon_k$$

$$\tau_l = \epsilon_l \mu_l ([\nabla V_l + (\nabla V_l)^T] - \frac{2}{3} \nabla \cdot V_l I)$$

$$\tau_k = \mu_k (\nabla V_k + (\nabla V_k)^T) + (\xi_k - \frac{2}{3} \mu_k) \nabla \cdot V_k I$$

where

$$G(\epsilon_k) = 10^{8.76 \epsilon_k - 0.27} \quad (\text{dynes/cm}^2)$$

$$\xi_k = \frac{4}{3} \epsilon_k^2 \rho_k d_k g_0 (1-e) \sqrt{\theta_k / \pi}$$

$$g_0 = (1 - (\epsilon_k / \epsilon_{k, \max})^{1/3})^{-1}$$

$$\mu_k = 5 \epsilon_k$$

Drag coefficients:

$$\beta_{lk} = \beta_{kl} = 150 \cdot \frac{\varepsilon_k^2 \mu_l}{\varepsilon_l (d_k \psi_k)^2} + 1.75 \cdot \frac{\rho_l \varepsilon_k |V_l - V_k|}{d_k \psi_k} \quad \varepsilon_l < 0.8$$

$$\beta_{lk} = \beta_{kl} = 0.75 C_D \frac{\varepsilon_k \varepsilon_l \rho_l |V_l - V_k|}{d_k \psi_k} \varepsilon_l^{-2.65} \quad \varepsilon_l \geq 0.8$$

$$\beta_{gs} = \beta_{sg} = \frac{3}{2} \alpha_{gs} (1+e) \frac{\rho_s \rho_g \varepsilon_s \varepsilon_g (d_s + d_g)^2}{\rho_s d_s^3 + \rho_g d_g^3} |V_s - V_g|$$

where

$$C_D = \frac{24}{Re_k} (1 + 0.15 Re_k^{3.687}) \quad Re_k < 1000$$

$$C_D = 0.44 \quad Re_k \geq 1000$$

$$Re_k = \frac{\varepsilon_l \rho_l |V_l - V_k| d_k \psi_k}{\mu_l} \quad k = g, s \quad \alpha_{gs} = 0.5$$

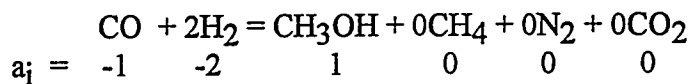
SPECIES BALANCE: FOR GAS AND LIQUID PHASE:

$$\frac{\partial}{\partial t} (\varepsilon_g \rho_g Y_i) + \nabla \cdot (\varepsilon_g \rho_g V_g Y_i) = \frac{\bar{a}_i \varepsilon_s \rho_s M_i r}{3.6 \times 10^6} - \varepsilon_l M_i R_i$$

$$\frac{\partial}{\partial t} (\varepsilon_l \rho_l X_i) + \nabla \cdot (\varepsilon_l \rho_l V_l X_i) = \varepsilon_l M_i R_i$$

$$\sum y_i = 1$$

$$\sum x_i = 1$$



By solving above equations simultaneously, we can obtain the following variables changing with time and position in a 2-D reactor:

$$\varepsilon_g, \varepsilon_l, \varepsilon_s, u_g, u_l, u_s, v_g, v_l, v_s, x_i, y_i$$

REACTOR'S OPERATING CONDITIONS: (see Fig 1 and Table 1 and 2)

2-D reactor	22.5"x320"
pressure	753.2 psig
temperature	250.3 °C
gas velocity	15.24 cm/s
catalyst density	3.011 g/cm ³
catalyst diameter	50 micrometer
liquid density	0.70025 g/cm ³
gas type	CO-rich.

SIMULATION:

The initial state of the reactor is shown in Fig 1 and Table 1. The gas phase consists of the inert N₂ only. At time zero, the syn-gas is injected to reactor through six orifices and the gas velocity is increased gradually to the final value during the first computing second. The values of all variables for each cell are stored every 0.05 seconds. After two weeks the program stopped at computing time of 35s because of the capacity limit of the hard disk. Then we continued the run by using a restart technique. This report is based on the results of the first 35 seconds.

ANALYSIS AND DISCUSSION:

Fig 2 shows the system output (or gas flowrate at the outlet) varying with time and the frequency response. There are strong oscillations occurring during the first 2.5 seconds. After that, a hydrodynamic steady state could be assumed. The two frequency peaks represent the system's oscillating frequency. To check the hydrodynamic model it is better to compare the frequency with the histogram of the LaPorte's RUN E-8.1.

The PCSHOW movie shows the volume fractions of gas, liquid and solid changing with time and the fast propagation of methanol concentration in the very early time. In Fig 3 we can see the mixing of the three phases when gas is injected at 0.5s. Fig 5 shows the shapes of the three phases at 5s. These shapes stay constant to 35s without a significant change. This phenomena matches with Fig 2 and supports the above steady state assumption. Fig 6a shows the propagation with the injection of syn-gas and Fig 6(b), 6(c) show the methanol concentration profiles at time 2.5s and 5.0s. The yellow area of Fig 6(c) keeps expanding very slowly with time. Since the N₂ fills the whole reactor before the injection of syn-gas, a very long time is needed to fill the reactor with syn-gas and methanol.

Fig 7, 8 and 9 show that the transient flow patterns of the gas phase do not change significantly during hydrodynamic steady state period. There is circulation inside the reactor, particularly in the lower area due to the non-uniform distribution of the orifices and wall effectiveness.

Fig 10 shows the time average volume fractions of gas, liquid and solid along the reactor's height. The slurry level and catalyst concentration are pretty close to LaPorte's measurements (see Table 1).

Fig 11 shows the composition profiles in gas phase for the lower area in which the distribution of methanol, in view of the PCSHOW movie, looks like it has reached steady state in chemical reaction sense. The rate of methanol production in Table 2 is estimated based on Fig 10 and average velocity in y-direction.

The final results will be submitted upon completion of the simulation.

Table 1. The reactor's compositions of initial setting, steady state and RUN E-8.1

	range 1	range 2	range 3
initial	0-72"	72"-168"	168"-320"
gas(%)	0.050	0.050	1.000
liquid(%)	0.426	0.950	0.000
solid(%)	0.524	0.000	0.000
	range 1	range 2	
steady state	0-184"	184"-320"	
gas(%)	0.170	1.000	
liquid(%)	0.670	0.000	
solid(%)	0.160	0.000	
	range 1	range 2	
Run E-8.1	0-196"	196"-300"	
gas(%)	0.295	1.000	
liquid(%)	0.555	0.000	
solid(%)	0.150	0.000	

Table 2 Gas compositions and methanol production

vol %	CO	CO ₂	H ₂	N ₂	CH ₃ OH
inlet	51	13	35	1	0
lower area	51	14	25.5	1.5	8
	CO conv. (%)	Total Catalyst (kg)	MeOH(gmol/h/kg)	Net MeOH(TPD)	
lower area *	13.53	740	14.59	8.267	
RUN E-8.1	13.50	567	20.50	10.03	

* Estimation based on the results of the lower area (height = 0--120")

NOTATION

a ----interfacial area per unit volume(cm^2/cm^3)
 C_i^L ----concentration of i in bulk liquid phase ($\text{mole}/\text{cm}^3\text{-L}$)
 C_i^{g-L} ----concentration of i in G-L interface($\text{mole}/\text{cm}^3\text{-L}$)
 C_D ----drag coefficient
 d_i ----diameter of solid/gas bubble
 e ----restitution coefficient
 g_0 ----radial distribution function
 H_i ----Henry's constant of i ($\text{bar m}^3/\text{mole}$)
 $K_{L,i}$ ----mass transfer coefficient of i in L-phase(cm/s)
 \dot{m}_k ----rate of generation of phase k ($\text{g}/\text{cm}^3/\text{s}$)
 M_i ----molecular weight of component i (g/mole)
 P ----pressure
 r ----rate of reaction($\text{mole}/\text{kg-cat.}/\text{hr}$)
 R_i ----rate of mass transfer($\text{mole}/\text{cm}^3/\text{s}$)
 Re_k ----Reynolds number
 T ----temperature(K)
 u, v ----velocity in x, y -direction(cm/s)
 V ----velocity vector(cm/s)
 x_i ----weight fraction of i in liquid phase
 y_i ----weight fraction of i in gas phase

Greek letters:

α_i ----stoichiometric coefficient of i
 β ----frictional coefficient
 ϵ ----volume fraction
 ρ ----density(g/cm^3)
 μ ----viscosity
 θ ----granular temperature
 τ ----shear stress
 ψ ----sphericity of solid/gas bubble
 ξ ----bulk viscosity

Subscripts:

g, l, s ----gas, liquid, solid respectively
 i ----species
 k ----solid or gas

REFERENCE:

Air Products and Chemicals, Inc., "Liquid-Entrained Catalyst Operations at LaPorte Methanol Process 1984-1985", Final Report to DOE for Contract No. DE-AC-22-81PC300019 (1987)

Air Products and Chemicals, Inc., "Liquid Phase Methanol LaPorte Process Development Unit: Modification, Operation, and Support Studies.", Draft Report to DOE for Contract No. DE-AC22-87PC90005 (1991).

Air Products and Chemicals, Inc. " Synthesis of Dimethyl Ether and Alternative fuels in the Liquid Phase from Coal-Derived Synthesis Gas.", Topical Report to DOE for Contract No. DE-AC22-90PC89865 (1992).

D. Gidaspow, "Multiphase Flow and Fluidization--Continuum and Kinetic Theory Descriptions," Academic Press (1994b)

G.H. Graff, J.G.M. Winkelman, E.J. Stamhuis and A.A.C.M. Beenackers, "Kinetics of the Three-Phase Methanol Synthesis," Chem. Eng. Sci., Vol. 43, No. 8, P.2161-68 (1988)

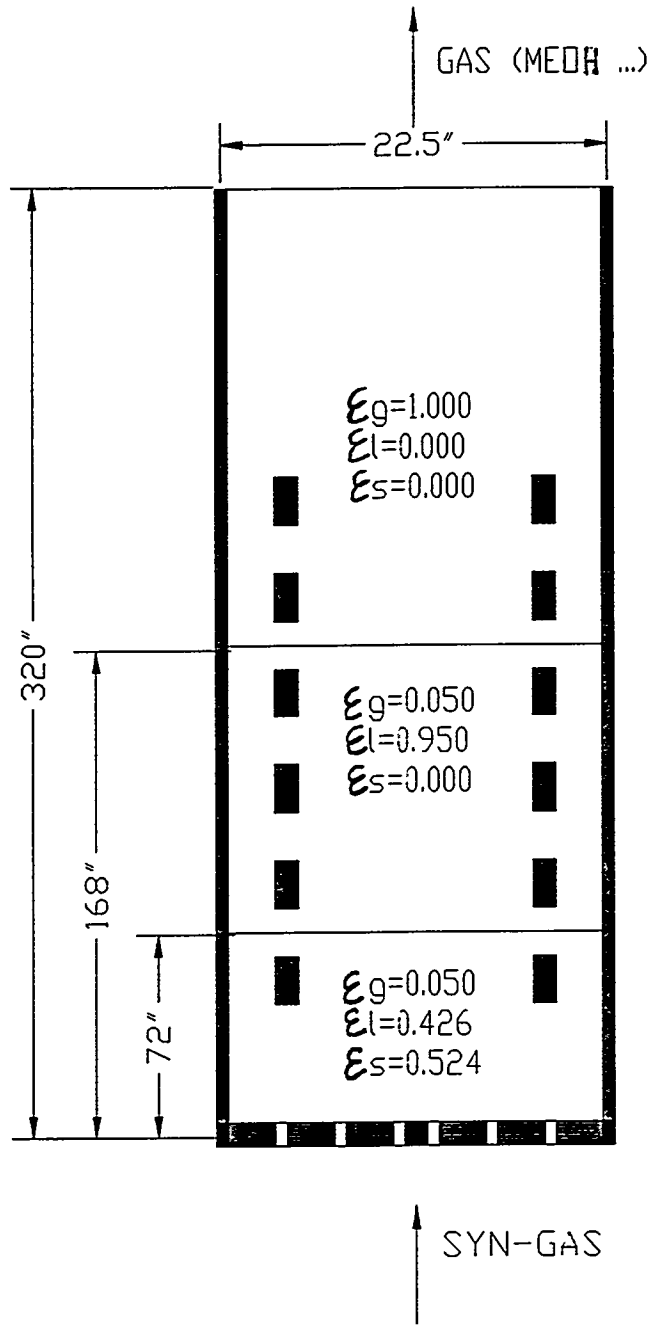
S. Ledakowicz, H. Nettelhoff and W.D. Deckwer, "Gas-liquid mass transfer data in a stirred autoclave reactor", Ind. Engng. Chem. Fundam., 23, 510-512(1984)

Viking Systems International, "Design of Slurry Reactor for Indirect Liquefaction Applications"

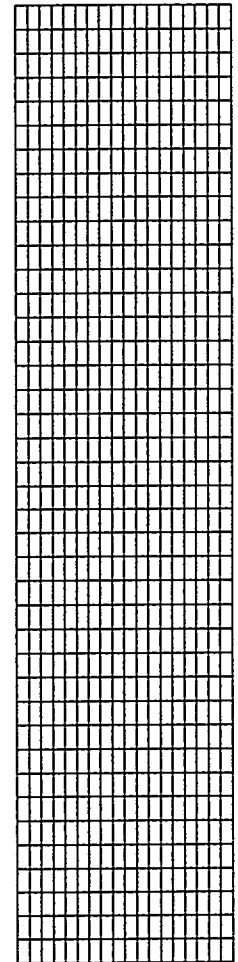
W.V. Wedel, S. Ledakowicz and W.D. Deckwer, "Kinetics of Methanol Synthesis in the Slurry Phase", Chem. Eng. Sci., Vol.43, No. 8, P. 2169-74 (1988)

Y. Wu and D. Gidaspow, "Hydrodynamic Models for Slurry Bubble Column", 1st Technical Progress Report to DOE for Contract No. DE-FG22-94PC94208 (1994a).

Fig. 1 Reactor and grid



The grid is the right half of the reactor.



grid 18x40
dx=0.7"
dy=8"

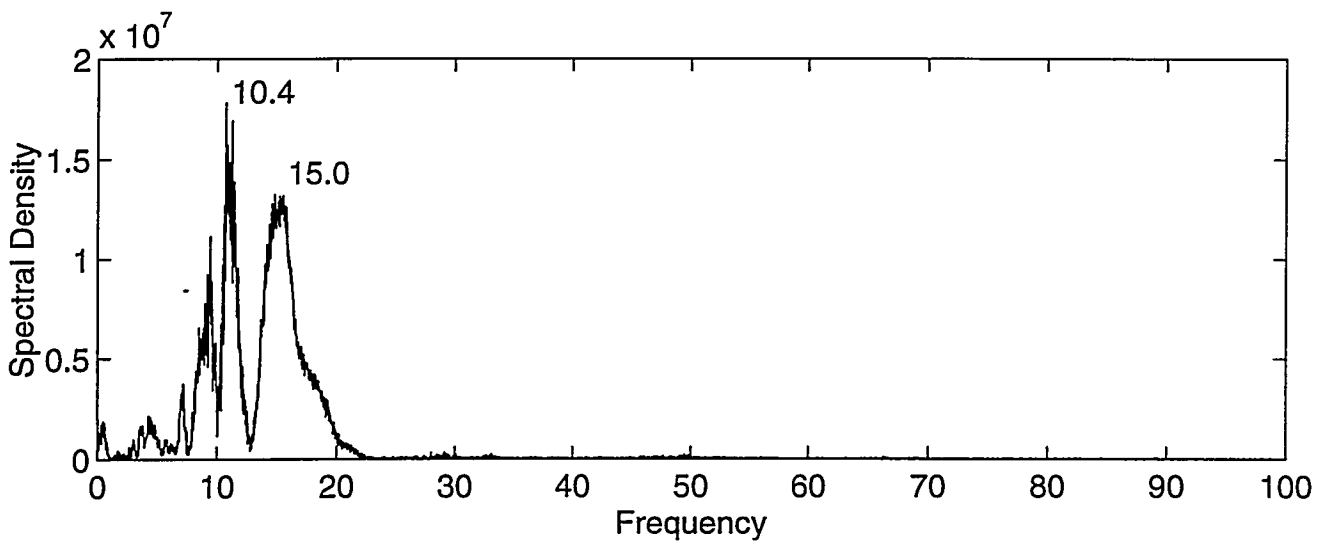
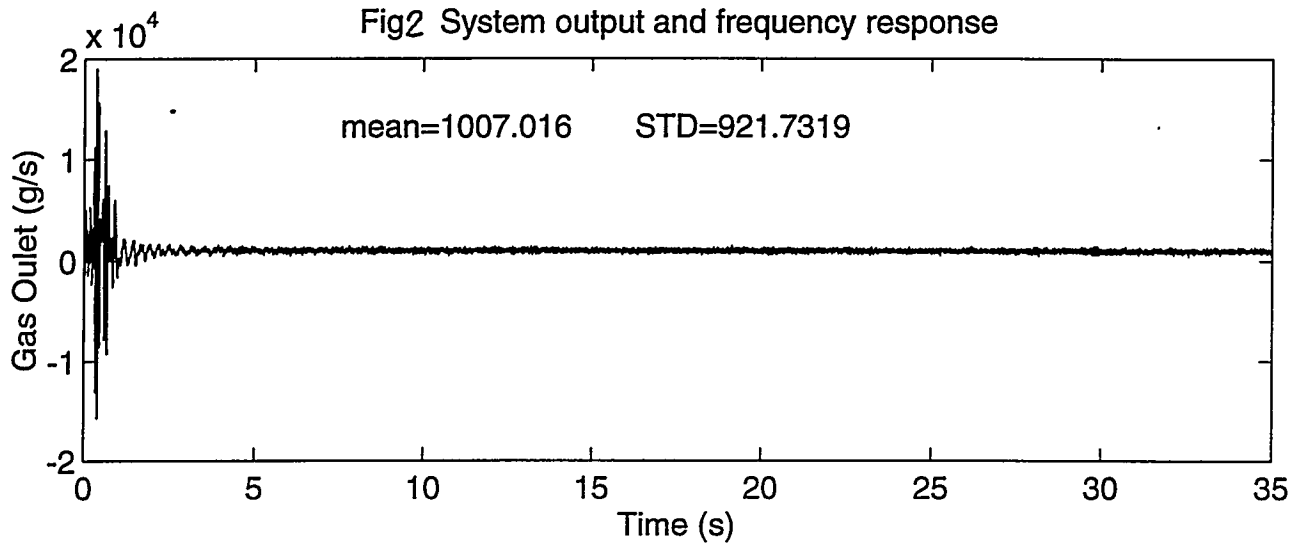


Fig. 3 The volume fraction profiles of gas, liquid and solid at time = 0.5s.

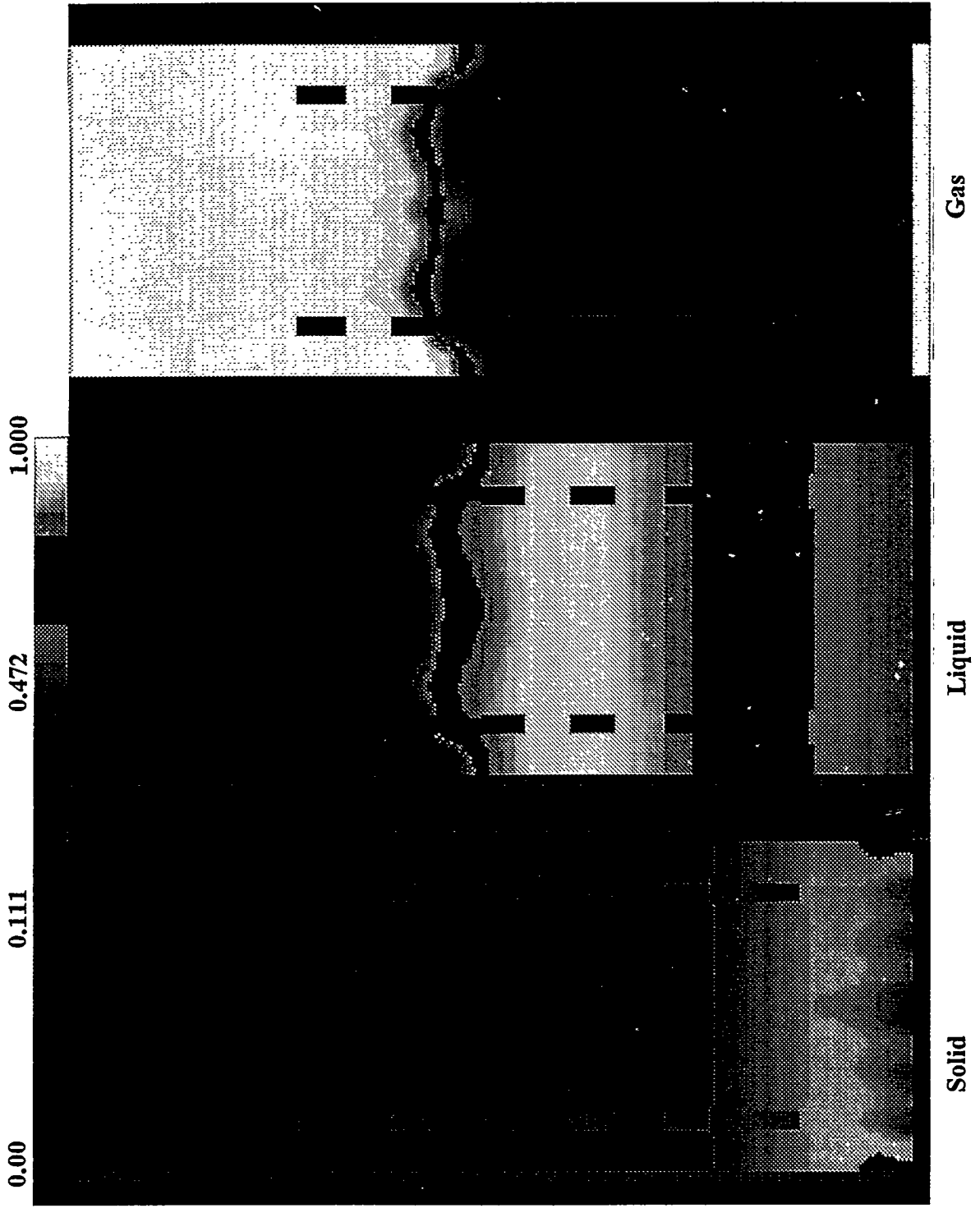


Fig. 4 The volume fraction profiles of gas, liquid and solid at time = 2.5s.

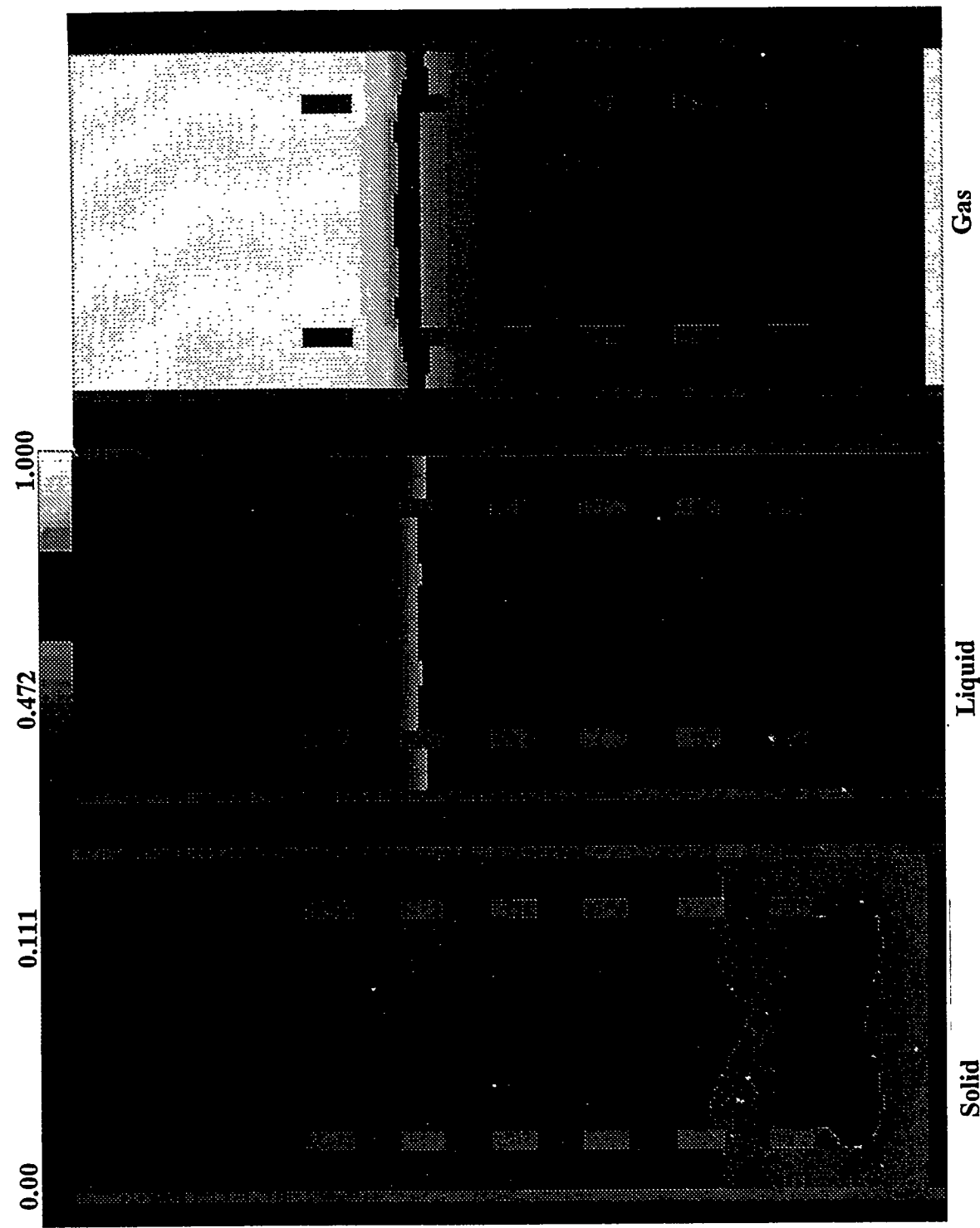


Fig. 5 The volume fraction profiles of gas, liquid and solid at time = 5s.

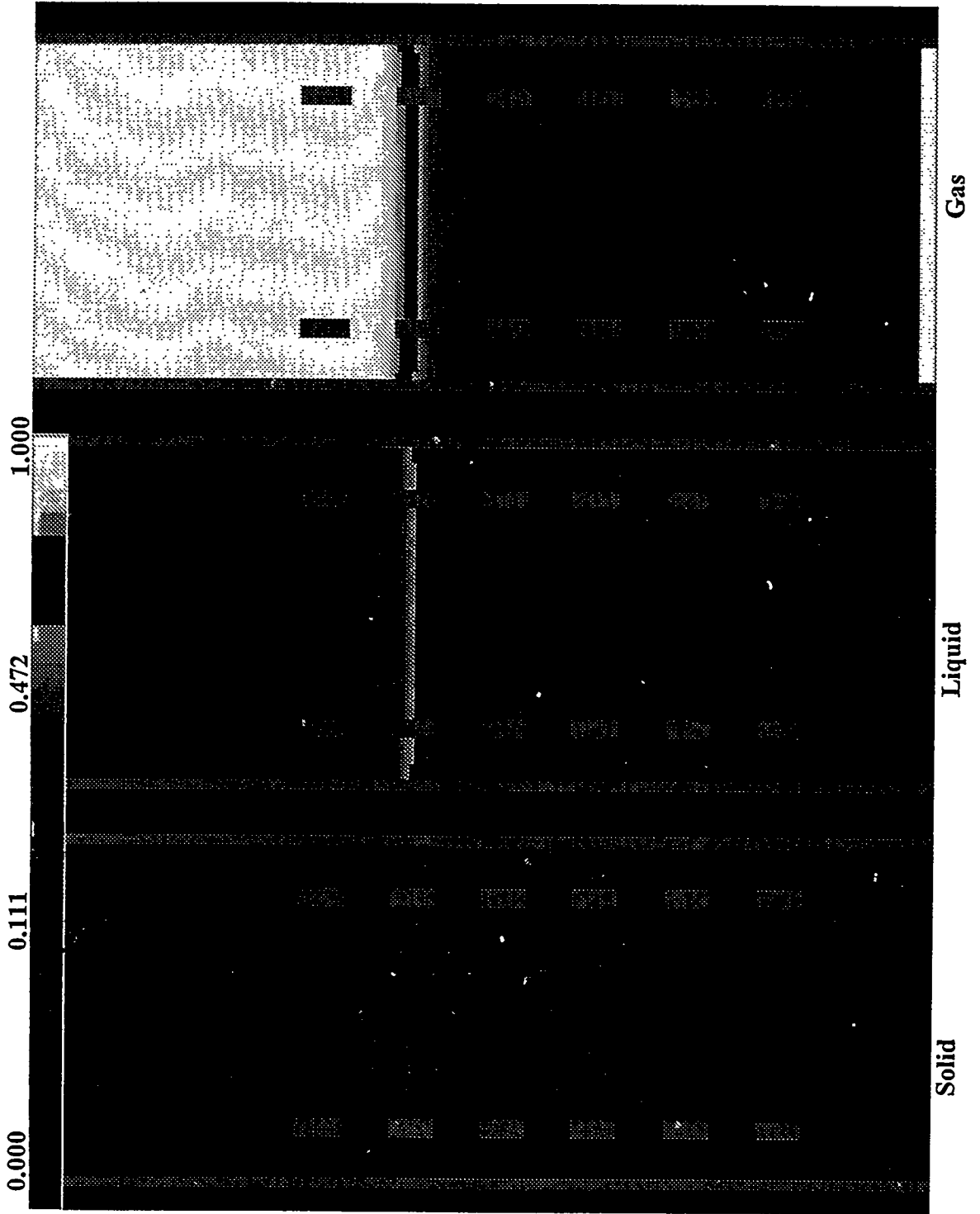
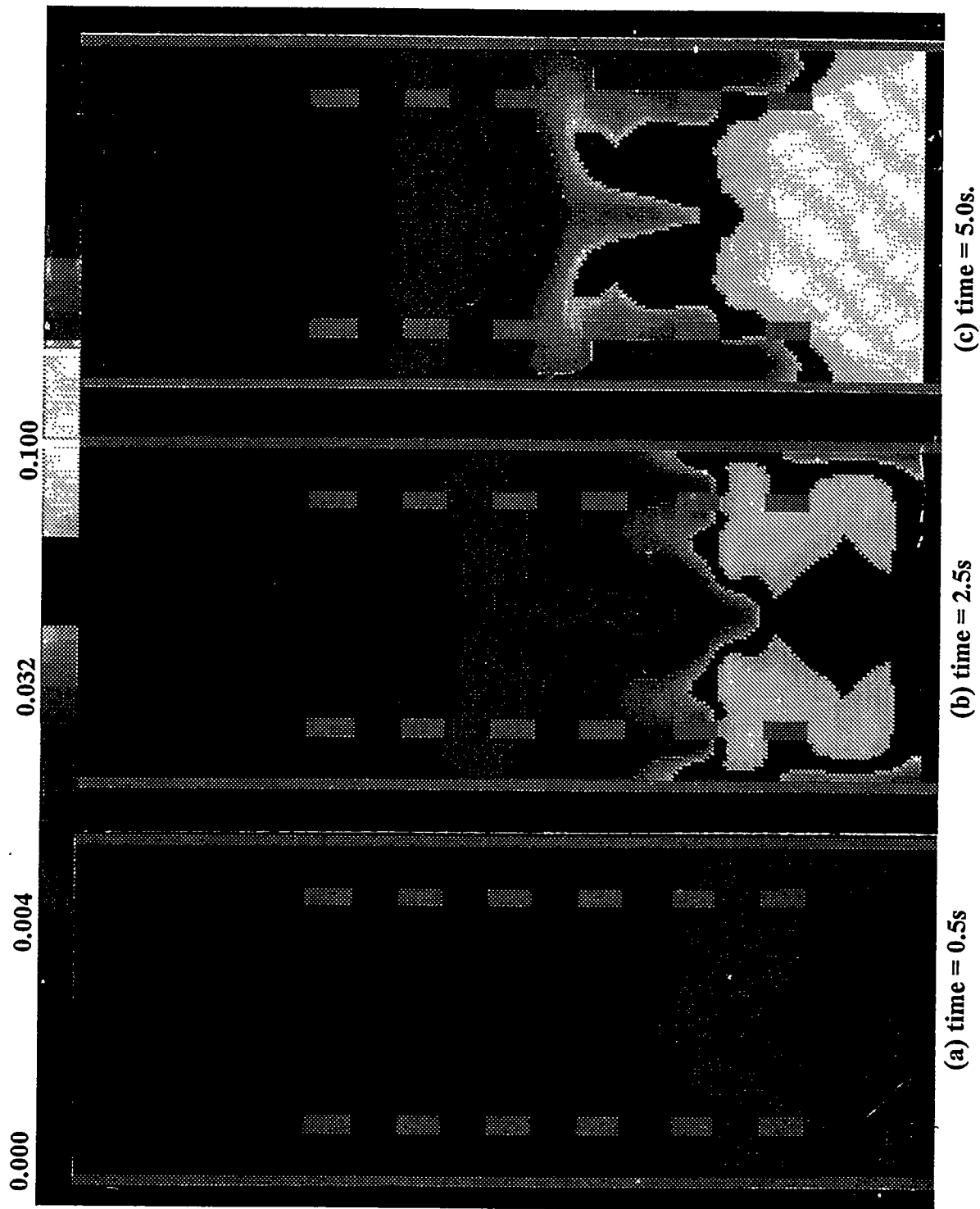


Fig. 6 The methanol concentration profiles in gas phase (mole fraction).
(a) time = 0.5s, (b) time = 2.5s, (c) time = 5.0s.



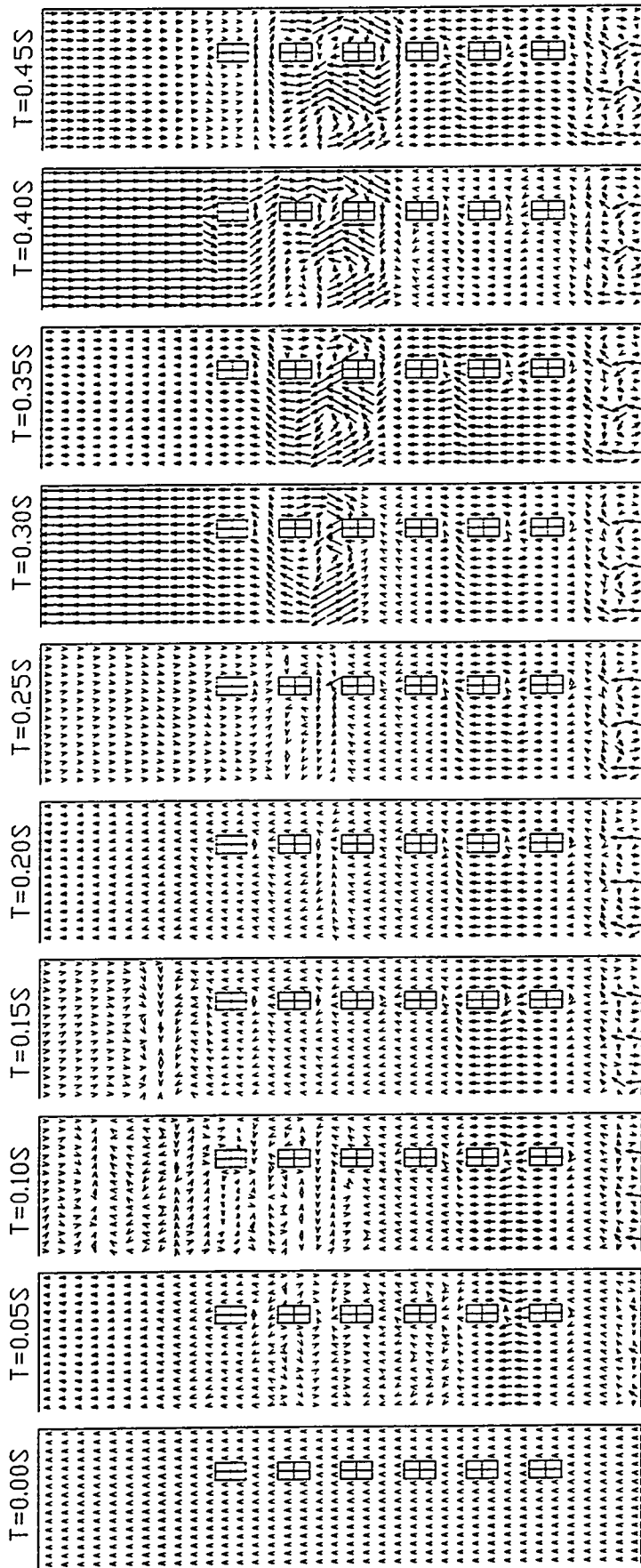


Fig. 7 The transient gas flow pattern as a function of time.

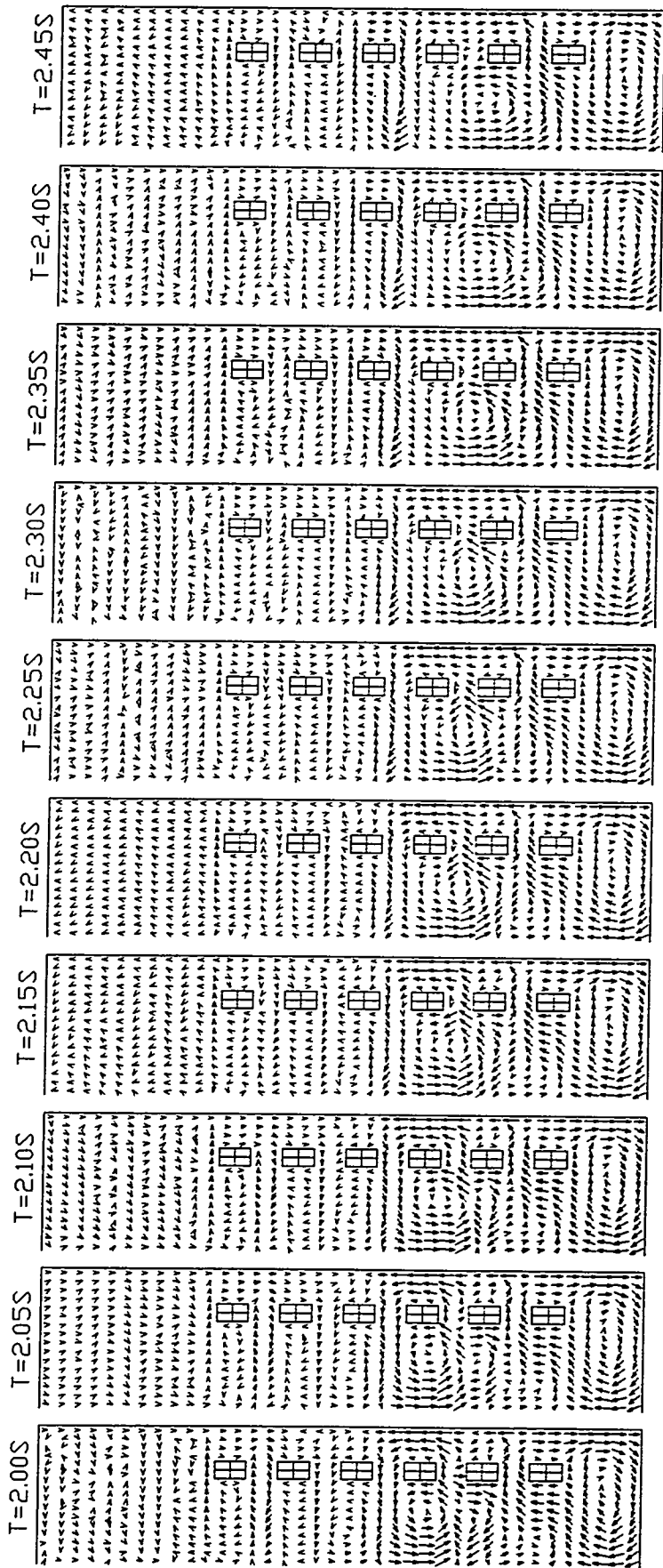


Fig. 8 The transient gas flow pattern as a function of time.

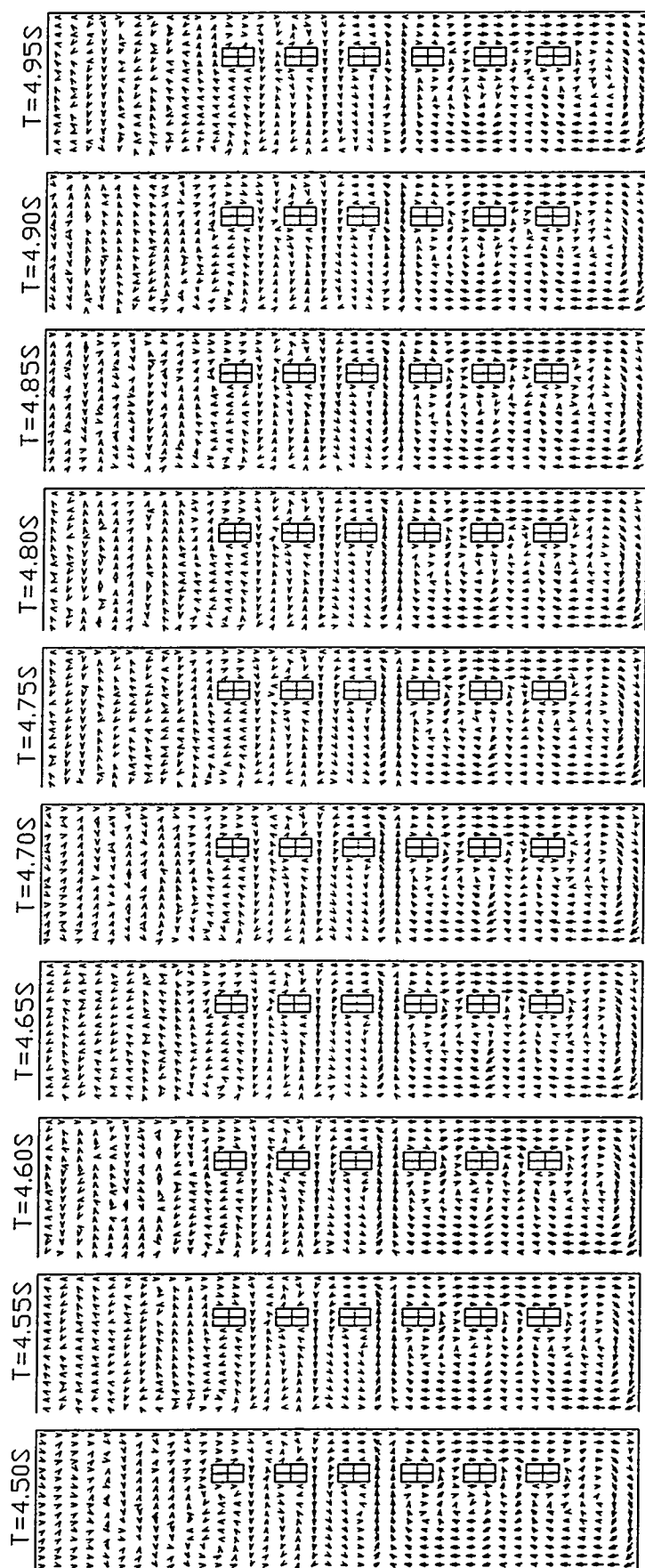


Fig. 9 The transient gas flow pattern as a function of time.

